Cell Reports, Volume *23*

Supplemental Information

Functional Genome-wide Screen Identifies Pathways Restricting Central Nervous System Axonal Regeneration

Yuichi Sekine, Alexander Lin-Moore, Devon M. Chenette, Xingxing Wang, Zhaoxin Jiang, William B. Cafferty, Marc Hammarlund, and Stephen M. Strittmatter

SUPPLEMENTAL MATERIALS

Supplemental Experimental Procedures
Supplemental Figures S1-S6

SUPPLEMENTAL EXPERIMENTAL PROCEDURES

Resource Table

REAGENT or RESOURCE	SOURCE	IDENTIFIER
Antibodies		
Mouse monoclonal anti-βIII-Tubulin antibody	Promega	#G7121
Rabbit polyclonal anti-Rab27b antibody	Immuno-Biological Laboratories	#18973
Rabbit monoclonal anti-PDGF Receptor α antibody	Cell Signaling Technology	#3174
Rabbit polyclonal anti-Iba1 antibody	Wako	#019-19741
Chicken polyclonal anti-NeuN antibody	abcam	#ab130414
Mouse monoclonal anti-O4 antibody	R&D systems	#MAB1326
Rabbit polyclonal anti-FLAG antibody	Sigma-Aldrich	#F7425
Mouse monoclonal anti-β-Actin antibody	Sigma-Aldrich	#A1978
Mouse monoclonal anti-GFAP antibody	Sigma-Aldrich	#G3893
Mouse monoclonal anti-GFP antibody	Santa Cruz Biotechnology	#sc-9996
Rabbit polyclonal anti-5HT antibody	Immunostar	#20080
Donkey anti-mouse IgG Alexa Fluor 488	Thermo Fisher Scientific	#A21202
Donkey anti-mouse IgG Alexa Fluor 647	Thermo Fisher Scientific	#A31571
Donkey anti-rabbit IgG Alexa Fluor 488	Thermo Fisher Scientific	#A21206
Goat anti-mouse IgM Alexa Fluor 488	Thermo Fisher Scientific	#A21042
Goat anti-Chicken IgG Alexa Fluor 488	Thermo Fisher Scientific	#A11039
Goat anti-Chicken IgG Alexa Fluor 568	Thermo Fisher Scientific	#A11041
IRDye 680 Donkey anti-Mouse IgG (H+L)	Li-Cor	#926-68072
IRDye 680 Donkey anti-Rabbit IgG (H+L)	Li-Cor	#926-68073
IRDye 800 Donkey anti-Rabbit IgG (H+L)	Li-Cor	#926-32213
IRDye 800 Donkey anti-Goat IgG (H+L)	Li-Cor	#926-32214
Chemicals, Peptides, and Recombinant Proteins		
Rhodamine Phalloidin	Thermo Fisher Scientific	#R415
Streptavidin Alexa Fluor 568	Thermo Fisher Scientific	#S11226
DAPI	Cell signaling Technology	#4083
Cholera Toxin Subunit B Alexa Fluor 555 Conjugate	Thermo Fisher Scientific	# C34776

AS1949490	Santa Cruz Biotechnology	#sc-358828
Dextran Biotin 10,000 MW Lysine Fixable (BDA-10,000)	Thermo Fisher Scientific	# D1956
Zymosan A	Sigma-Aldrich	#Z4250
Experimental Models: Organisms/Strains		
Mouse: *Rab27b*$^{-/-}$ mice	(Tolmachova et al., 2007)	N/A
C. elegans: oxIs12[Punc-47::GFP, lin-15+]	CGC	WormBase_ID:EG1285
C. elegans: rab-27 (sa24); oxIs12[Punc-47::GFP, lin-15+]	This Study	XE1873
C. elegans: wpEx287[Punc-47::RAB-27::unc-54 3'UTR::SL2::mCherry]	This Study	XE1892
C. elegans: wpEx287[Punc-47::RAB-27::unc-54 3'UTR::SL2::mCherry];rab-27(sa24)	This Study	XE1890
C. elegans: rab-27 (sa699); oxIs12[Punc-47::GFP, lin-15+]	This Study	XE1910
Recombinant DNA		
pAAV-U6-GFP Expression Vector	Cell Biolabs	#VPK-413
pAAV-U6-shNC-GFP	This paper	N/A
pAAV-U6-shSocs4-GFP	This paper	N/A
pAAV-U6-shRab27b #1-GFP	This paper	N/A
pAAV-U6-shRab27b #2-GFP	This paper	N/A
pAAV-U6-shRPH3a #1-GFP	This paper	N/A
pAAV-U6-shRPH3a #2-GFP	This paper	N/A
pCDNA3.1+-DYK-Rab3b	GenScript	#OMu03928
pCDNA3.1+-DYK-Rab3c	GenScript	#OMu07534
pCDNA3.1+-DYK-Rab18	GenScript	#OMu17631
pCDNA3.1+-DYK-Rab27b	GenScript	#OMu18472
pCDNA3.1+-DYK-Rab31	GenScript	#OMu10080
pCDNA3.1+-DYK-Arf4	GenScript	#OMu00249
pAAV-CAG-GFP	addgene	#28014
pAAV-CAG-Rab3b T36N	This paper	N/A
pAAV-CAG-Rab3b Q81L	This paper	N/A
pAAV-CAG-Rab3c T44N	This paper	N/A
pAAV-CAG-Rab3c Q89L	This paper	N/A
pAAV-CAG-Rab18 S22N	This paper	N/A
pAAV-CAG-Rab18 Q67L	This paper	N/A
pAAV-CAG-Rab27b T23N	This paper	N/A
pAAV-CAG-Rab27b Q78L	This paper	N/A
pAAV-CAG-Rab31 S19N	This paper	N/A
pAAV-CAG-Rab31 Q64L	This paper	N/A
pAAV-CAG-Arf4 T31N	This paper	N/A
pAAV-CAG-Arf4 Q71L	This paper	N/A
Software and Algorithms		
MATLAB	Mathworks	http://www.mathworks.com/
GraphPad Prism7	GraphPad Software	http://www.graphpad.com/

IBM SPSS Statistics	IBM	https://www.ibm.com/us-en/marketplace/spss-statistics
Image J	NIH	https://imagej.nih.gov/ij/
DAVID	bioinformatical analysis	http://david.abcc.ncifcrf.gov/
Cytoscape	bioinformatical analysis	http://www.cytoscape.org/
BiNGO	bioinformatical analysis	http://apps.cytoscape.org/apps/bingo
GeneMania	bioinformatical analysis	http://genemania.org/
String	bioinformatical analysis	https://string-db.org/

CONTACT FOR REAGENT AND RESOURCE SHARING

Further information and requests for resources and reagents should be directed to and will be fulfilled by the Lead Contact, Stephen M. Strittmatter (stephen.strittmatter@yale.edu).

EXPERIMENTAL MODEL AND SUBJECT DETAILS

Mice

All animal studies were conducted with approval of the Yale Institutional Animal Care and Use Committee All mice were maintained on a 12 h light-dark schedule with access to standard mouse chow and water *ad libitum*. Both male and female mice were included as mice were collected from sequential littermates of the appropriate genotypes in tissue culture experiments. Spinal cord injury studies were performed only with female mice to facilitate bladder management. Both male and female mice were used of optic nerve crush studies. The age of mice is specified in each Figure legend, and for CNS injury was introduced at 10 weeks age. The *Rab27b*$^{-/-}$ mice (Tolmachova et al., 2007) were studied on the C57Bl6J background after >10 backcrosses, with WT C57Bl6J control mice.

METHOD DETAILS

Experimental Design

All behavioral measurements and all imaging quantifications were conducted by experimenters unaware of experimental group. No data were excluded from the analysis. Mice were collected sequentially from littermate cohorts without regard to sex or any characteristic other than the specified genotypes. The data from all observations were pooled by experimental group for statistical analysis. The n values are specified in each Figure legend, and reflect either separate mice or separate experimental batches as appropriate and as indicated. Sample sizes were determined to be comparable to previous studies that examined axonal regeneration amongst phosphatases.

Primary cortical neuron culture and Cortical Axon Regeneration Assay

Primary cortical cultures were established from E17 C57BL/6 mice or *Rab27b*$^{-/-}$ mice(Tolmachova et al., 2007). Cortices were dissected in ice-cold Hibernate E medium (catalog #HE-Ca; BrainBits) and incubated in digestion HBSS medium containing 30 U/ml Papain (catalog #LS003127; Worthington Biochemical), 1.5 mM $CaCl_2$, 2.5mM EDTA, and 2 mg/ml DNaseI (catalog #DN25; SIGMA) at 37°C for 20 min. Digested tissues were triturated and suspended in Neurobasal-A. Cells were plated on 96 well tissue culture plates coated with poly-D-lysine at a density of $2.5x10^4$ cells per well in 200 µl of Neurobasal-A media supplemented with B-27, GultaMAX, and penicillin-streptomycin (all from Invitrogen). Cortical axon regeneration assay was performed as described previously(Huebner et al., 2011). On DIV8, 96-well cultures were scraped using a floating pin tool with FP1-WP pins (V&P Scientific) and allowed to regenerate for another 48-60 h before fixing with 4% paraformaldehyde.

Regenerating axons in the scrape zone were visualized using an antibody against βIII tubulin (1:2000, mouse monoclonal; catalog #G712A; Promega). Growth cones were visualized by staining for F-actin using rhodamine conjugated phalloidin (1:2000, catalog #R415, Life Technologies). Cell density was visualized using nuclear marker DAPI (0.1µg/ml, catalog #4083, Cell Signaling Technology). Images were taken on a 10x objective in an automated high-throughput imager (ImageXpress Micro XLS, Molecular Devices) under identical conditions. Regeneration zone identification, image thresholding and quantitation were performed blind to conditions in Image J for general regeneration assay or using an automated MATLAB script for screening.

shRNA based regeneration screen

Mouse cortical neurons were cultured in 96 well tissue culture plates at a density of $2.5x10^4$ cells per well. On DIV 3, lentiviral particles targeting 16,007 mouse genes with 83,106 unique shRNA clones (Mission TM TRC Mouse Lentiviral shRNA Library 10180801; Sigma) were added to the neurons. Axon regeneration assay as described above was performed: on DIV 8, 96-well cultures were scraped and fixed on DIV 10.

Transfection

Cortical neurons were transfected using Amaxa mouse neuron nucleofector kit according to the manufacture's protocol. Before to plate, the dissected 4 x 10^6 cortical neurons were resuspended in 100 µl of nucleofector solution and mixed with 5 µg of plasmids. Then neurons were nuculeofected using the program 0-005 and plated on PDL-coated 96 well for regeneration assay, 24 well plate for western blot or 8 well glass chamber slide for confocal imaging.

Immunoblotting

Cell lysate or immunoprecipitated samples were resolved by SDS-PAGE and transferred to nitrocellulose membranes. Then, they were incubated in blocking buffer (Blocking Buffer for Fluorescent Western Blotting, Rockland MB-070-010) for 1 h at RT and immunoblotted with the appropriate primary antibodies. Following primary antibody incubation, secondary antibodies (Odyssey IRDye 680 or 800) were applied for 1 h at RT. Membranes were then washed and visualized using a Licor Odyssey Infrared imaging system.

Expression plasmids,

Wild-type mouse-Rab3b, Rab3c, Rab18, Rab27b, Rab31 and Arf4 were purchased from GenScript. Those clones were subcloned into pAAV-CAG-GFP vector using BamHI/EcoRI digestion and used for generating mutant constructs by PCR-methods using KOD Hot start DNA polymerase (TOYOBO, Japan) and sequenced. Following primers were used for making point mutation, Rab3b T36N, F-AGCAGCGTCGGGAAGAACTCCTTCCTTTTC, R-GAAAAGGAAGGAGTTCTTCCCGACGCTGCT, Rab3b Q81L, F-ATGGGACACAGCTGGGCTAGAGCGGTA, R-TACCGCTCTAGCCCAGCTGTGTCCCAT, Rab3c T44N, F-AGCAGCGTGGGCAAAAACTCTTTCCTGTTC, R- GAACAGGAAAGAGTTTTTGCCCACGCTGCT, Rab3c Q89L, F- CACAGCAGGCCTGGAAAGATACAGGACCAT, R-ATGGTCCTGTATCTTTCCAGGCCTGCTGTG, Rab18 S22N, F-GTGGGCAAGAACAGCCTGCTCCTGAGGTTC, R- GAACCTCAGGAGCAGGCTGTTCTTGCCCAC, Rab18 Q67L, F-GATACAGCTGGTCTAGAGAGGTTCAGAACA, R-TGTTCTGAACCTCTCTAGACCAGCTGTATC, Rab27b T23N, F-GACTCAGGAGTCGGGAAGAACACATTTCTCTATAGA, R-TCTATAGAGAAATGTGTTCTTCCCGACTCCTGAGTC, Rab27b Q78L, F-TTTGGGACACTGCTGGACTAGAGCGGTTCC, R- GGAACCGCTCTAGTCCAGCAGTGTCCCAAA Arf4 T31N, F- GGATGCTGCTGGCAAGAACACAATTCTGTA, R-TACAGAATTGTGTTCTTGCCAGCAGCATCC, Rab31 S19N, F-GGGGGTTGGGAAAAACAGCATTGTGTGTCG, R- CGACACACAATGCTGTTTTTCCCAACCCCC, Rab31 Q64L, F- ATCTGGGACACCGCTGGCCTGGAG, R- CTCCAGGCCAGCGGTGTCCCAGAT, Arf4 Q71L, F- ATGGGATGTTGGTGGTCTAGATAAAATTAGGCC, R-GGCCTAATTTTATCTAGACCACCAACATCCCAT. pAAV-U6-GFP Expression Vector (#VPK-413, Cell Biolabs) was used for making shRNA constructs. Targeting shRNA sequences are shNC:TTCTCCGAACGTGTCACGT, shSocs4: GCTAATCTATGCTATCAGTAT,

shRab27b#1:GCATACCATACTTCGAAACAA, shRab27b#2:CTCTATAGATACACAGACAAT, shRPH3a#1:CATTGGCAAGTCTAATGATTA and shRPH3a#2:GACATTGGCAAGTCTAATGAT.

RT-PCR and Quantitative PCR

Total RNA from mouse cortex, spinal cord and retina were prepared according to the TRIzol Reagent protocol (SIGMA) and subjected reverse transcriptase (RT)-PCR using the M-MuLV Reverse Transcriptase (New England BioLabs). cDNA of each sample was then used for real-time qPCR with iQ supermix (BioRad) and TaqMan Gene Expression Assay (#Mm00469997 for rab27a, #Mm01262250 for rab27b, and #Mm99999915 for Gapdh from Applied Biosystem) on a Bio-Rad CFX Connect Real-Time PCR Detection System using standard cycles. Each sample was loaded in triplicates.

Immunocytochemistry

At DIV 8 neurons were scraped with pipet tip and allowed for 2 days to regenerate. Then, cells were fixed with 4% paraformaldehyde for 15 min, and then permeabilized with 0.1% Triton X-100 in PBS for 15 min. Regenerating axons in the scrape zone were visualized using an antibody against βIII tubulin (1:2000, mouse monoclonal; catalog #G712A; Promega). FLAG-Rab27b TN or QL were stained with anti-FLAG (1:1,000, Sigma-Aldrich, #F7425) antibody. Then, either Alexa-488 conjugated donkey anti-rabbit IgG and Alexa-647 conjugated donkey anti-mouse IgG (1:2,000, all from Invitrogen) were used to detect primary antibodies. Growth cones were visualized by staining for F-actin using rhodamine conjugated phalloidin (1:2000, catalog #R415, Life Technologies). Samples were mounted with mounting solution (Vector Laboratories) and observed using a LSM710 confocal microscope. Obtained pictures were analyzed using Image J.

C. elegans and laser axotomy studies

C. elegans were fed *Escherichia coli* OP50 and maintained on nematode growth media (NGM) plates at 20° C. For transgenic animals with extrachromosomal arrays, the relevant constructs were injected(Mello and Fire, 1995; Mello et al., 1991). The concentration of the injected plasmid *Punc-47::rab-27::unc-54 3'UTR::SL2::mCherry* into both N2 and *rab-27(sa24)* animals was 15ng/μL. *Pmyo-2::mCherry* was delivered at 2ng/μL as an injection marker. Transgenic worms were selected based on *Pmyo-2::mCherry* expression and visible soluble mCherry in GABA neurons. Laser axotomy was performed on late L4 *C. elegans* larvae as previously described (Byrne et al., 2011). All animals were imaged to visualize regeneration after twenty-four hours using an Olympus DSU mounted on an Olympus BX61 microscope, Hamamatsu ORCA-Flash4.0 LT camera, and Xcite XLED1 light source with BDX, GYX and RLX LED modules. Axons were scored for regeneration based on the amount of regrowth relative to the distance between the ventral and dorsal nerve cords. Significance is indicated with an asterisk (* $p<0.05$, Kolmogorov-Smirnov test).

Mice and surgery

All procedures and postoperative care were performed in accordance with the guidelines of the Institutional Animal Use and Care Committee at Yale University. Age matched adult (10 weeks) C57BL/6 wild-type female mice or *Rab27b*$^{-/-}$ (Tolmachova et al., 2007) were subjected to dorsal hemisection as described previously (Zou et al., 2015). All animals received subcutaneous injection of buprenex (0.01 mg/kg) 30 minutes before surgery and were deeply anesthetized with ketamine (100 mg/kg) and xylazine (15 mg/kg). To expose the dorsal spinal cord at T6 and T7 levels, laminectomy was performed. Dura mater was pierced and 1% lidocaine was dropped on the exposed cord for 1 min. Then a pair of microscissors was used to lesion the spinal cord to a depth of 1.0 mm to completely sever the dorsal and dorsolateral corticospinal tract (CST). Lateral aspect of the spinal cord was scraped with a 30-gauge needle to ensure completeness of the lesion. Muscle and skin overlying the lesion were sutured. All animals received subcutaneous injection of 100 mg/kg ampicillin and 0.1 mg/kg buprenex twice a day for the first two days after surgery, and additional injections later on as necessary. To trace the CST, biotin dextran amine (BDA) was injected bilaterally into the sensorimotor cortex 8 weeks after hemisection. In each animal, 75 nl of 10 % solution of BDA was injected at each of the six sites (coordinates from bregma in mediolateral/anterior–posterior format in mm: 1.0/0.0, 1.5/0.5, 1.5/0.5, 1.5/1.0, 1.0/-1.5, 1.5/-0.5) for a total of 450 nl volume per hemisphere. Two weeks after the tracing, animals were killed by transcardial perfusion with PBS followed by 4% PFA.

For optic nerve crush Injury study, both male and female C57BL/6J mice or *Rab27b*$^{-/-}$ mice were anesthetized by intraperitoneal injection of a cocktail of ketamine (100 mg/kg) and xylazine (10 mg/kg).

AAV serotype 2/2 was produced and purified >$1x10^{12}$ genome copies per milliliter, and 1.5 µl of control or shSocs4 virus was injected intraorbitally to WT animals at 2 weeks prior to crush surgery. Topical 2% lidocaine anesthetic was applied to the eyeball, and then the optic nerve was exposed intraorbitally with care taken to avoid damage to the ophthalmic artery. The nerve was injured by crushing with a jeweler's forceps (Dumont 5; Fine Science Tools) for 5 s at a location 1 mm posterior to the eyeball (Wang et al., 2015). For intraocular injection of Zymosan, 2 µl of suspension (10 mg/ml in saline) was injected right after injury. Alexa-555-Cholera toxin beta (CTB) was injected intravitreally to trace retinal ganglion cell axons 14 days after injury. Three days after the tracing, animals were sacrificed and dissected the optic nerves.

Behavioral test

Surgery and behavioral tests were performed unaware of the genotype of the mice. For mouse behavioral observation, the Basso Mouse Scale (BMS) was used as a measure of open-field locomotion(Basso et al., 2006), which has a quantitative scale from 0 to 9. Animals were tested 3 d before dorsal hemisection for baseline function and 3, 7, 14, 21, 28, 35, 42, 49, 56, 63 and 70 d post lesion (dpl). RotaRod test (48 dpl) was used as a measure of motor coordination. The rotarod apparatus (Columbus Instruments, Columbus, OH) was set at a baseline speed of 2 rpm, with acceleration at 0.2 rpm/sec. Latency for the animal to fall off the rotating drum was recorded. The average time was calculated from five consecutive trials in each session. Grid-walking test (55 dpl) was performed previously(Starkey et al., 2005). Mice were placed on an elevated 300 mm x 200 mm metal grid with 10 mm x 10 mm square space and allowed to freely explore the grid for 3 min. Mice were videotaped via reflection from mirror placed under the grid and scored for the percentage of impaired steps out of the first 50 steps taken with left and right hind limbs individually. Impaired steps were scored that the limb fell between the rungs or an incorrectly placed step where either the ankle or tips were placed on the rungs without proper grasping, or when the limb was correctly placed but slipped off during weight bearing.

Histology and immunohistochemistry

All histological and axon counting were performed by an observer unaware of animal genotype. Mice were euthanized and transcardially perfused with cold PBS followed by 4% paraformaldehyde. Spinal cords were dissected, postfixed in 4% paraformaldehyde at 4°C, and subsequently embedded in 10% gelatin. Serial sections (40 µm) were collected on a vibratome (VT1000S, Leica). Transverse sections were collected at cervical enlargements and lumbar enlargements. Thoracic lesion site (from -5mm rostral to +5mm caudal) was excised from each animal and sectioned sagittally, collecting every single section. Sections of spinal cord were blocked and permeabilized with 10% normal donkey serum and 0.3% Triton X-100 in PBS for 1h. Then, sections were incubated with 5-HT (1:1,000) or anti-GFAP (1:1,000) antibody and visualized with Alexa-488 conjugated secondary antibody (1:1,000). The images were analyzed by using National Institutes of Health (NIH) ImageJ 1.49v, as described previously (Wang et al., 2014). For analysis of serotonin innervation, immunoreactive serotonin fibers in the ventral horn of transverse sections were selected by thresholding, and then the intensity of serotonin fiber per area was measured after using the ''skeletonize'' function.

For traced CST axon analysis, every other sequential 40 µm sagittal section of spinal cord tissue extending from 5 mm rostral to 5 mm caudal to the injury was stained with Alexa Fluor568. Labeled axons crossing dorsal ventral lines at 100 µm intervals from the injury epicenter defined by anti-GFAP staining were counted, summed and multiplied by two to correct for sampling every other consecutive section.

For optic nerve (ON) studies, the ON was dissected from the eyeball and postfixed in the 4% PFA solution. After clearing the whole nerve by using a clearing procedure(Erturk et al., 2011), the sample was whole-mounted on a glass side with a coverslip for imaging. For ON axon quantification, the ON was imaged by using the Zeiss LSM 710 confocal microscope with 20 x lens. Axons labeled with CTB were counted from the different distances to the crush lesion. Total number of regenerating axons was counted from each image in 30-40 z-stacks.

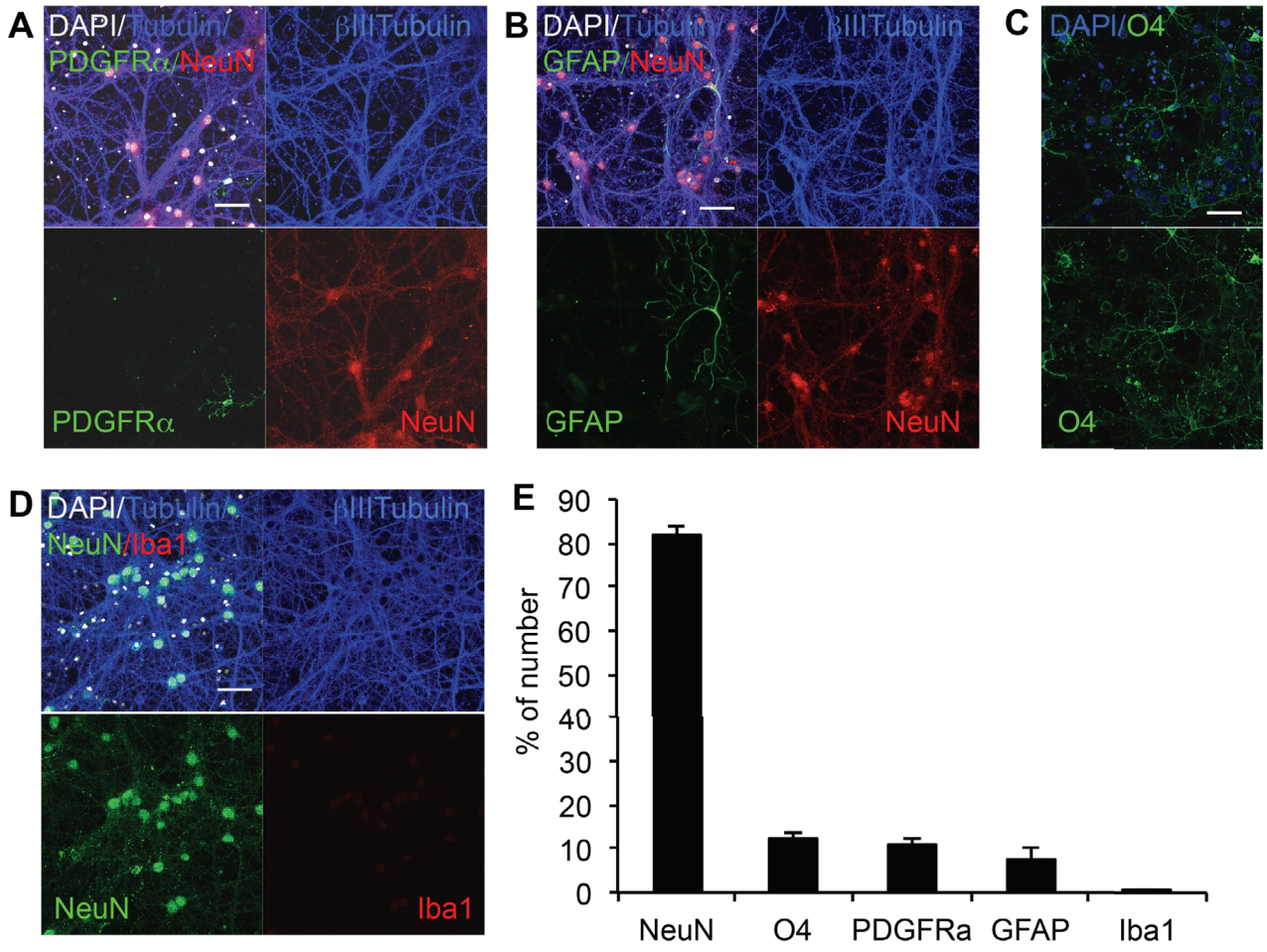

Figure S1. Assessment of Cell Type Abundance in Primary Cortical Culture at DIV 10 (Related to Figure 1).

(A-D) At DIV 10 primary cultures of E17 cortices were stained with indicated antibodies. Most cells are NeuN positive, while there are few NeuN-negative cells which are positive for PDGFRα, GFAP or O4. Scale bars represent 100 μm.

(E) The graph shows the percentage of cells positive for each marker as a fraction of DAPI-positive cells. Mean±SE, n=10 from randomly taken pictures.

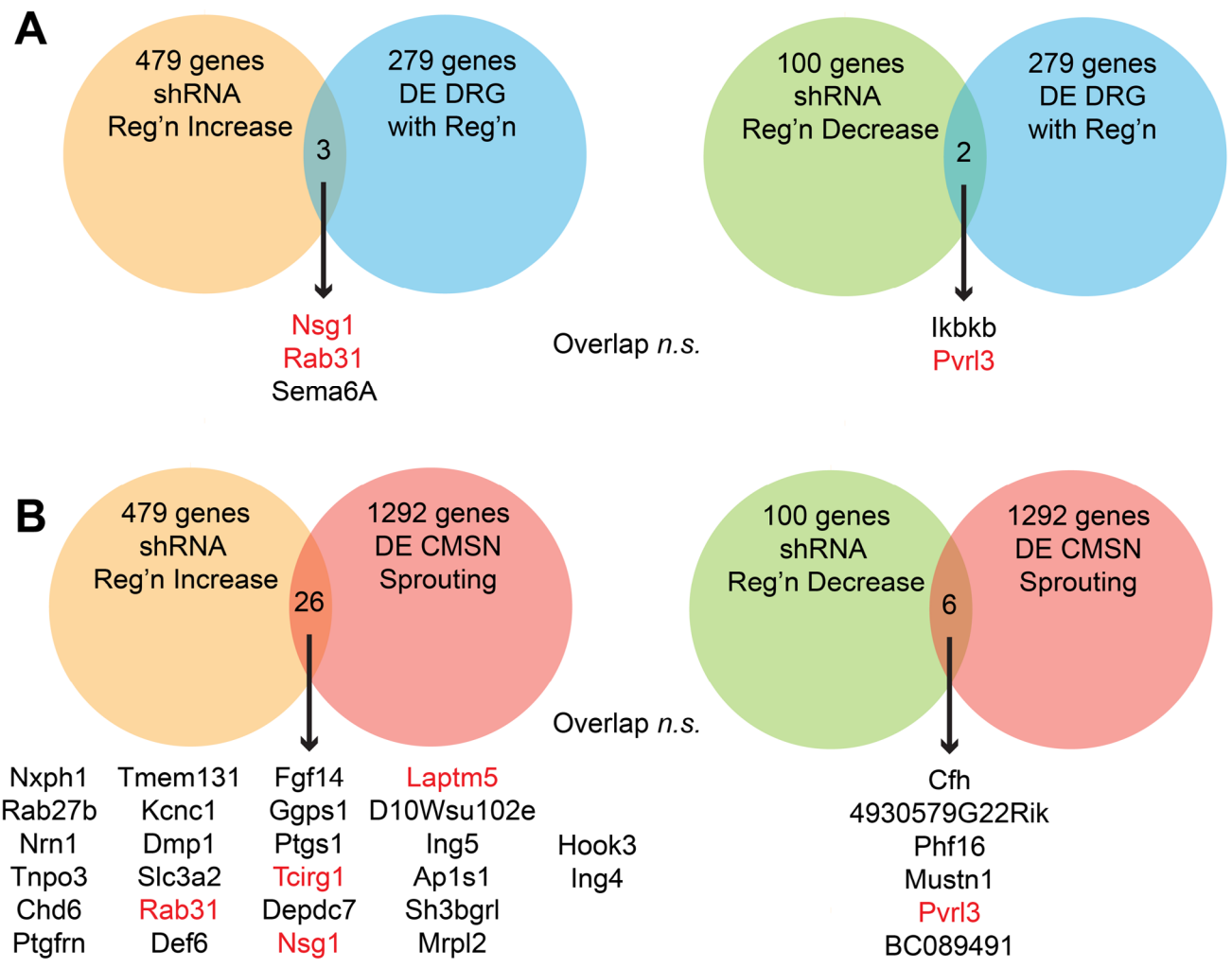

Figure S2. Comparison of Functional Axon Regeneration Genes with Repair-Related Expression Profiles (Related to Figure 2).

(A) The functional axonal regeneration gene list from Figure 1 was compared to the list of 279 genes differentially expressed in DRG one week after sciatic nerve axotomy (Tanabe et al., 2003). The genome-wide significance of the overlap between lists was compared by Chi-square test, $P > 0.05$. Individual genes present in both data sets are listed. Genes in red were also detected in other comparisons from Fig. 2 or Suppl. Fig. S1.

(B) The functional axonal regeneration gene list from Figure 1 was compared to the list of genes differentially expressed in sprouting cortico-spinal motoneurons 4 weeks after pyramidotomy (Fink et al., 2017). The genome-wide significance of the overlap between lists was compared by Chi-square test, $P > 0.05$. Individual genes present in both data sets are listed. Genes in red were also detected in other comparisons from Fig. 2 or Suppl. Fig. S1.

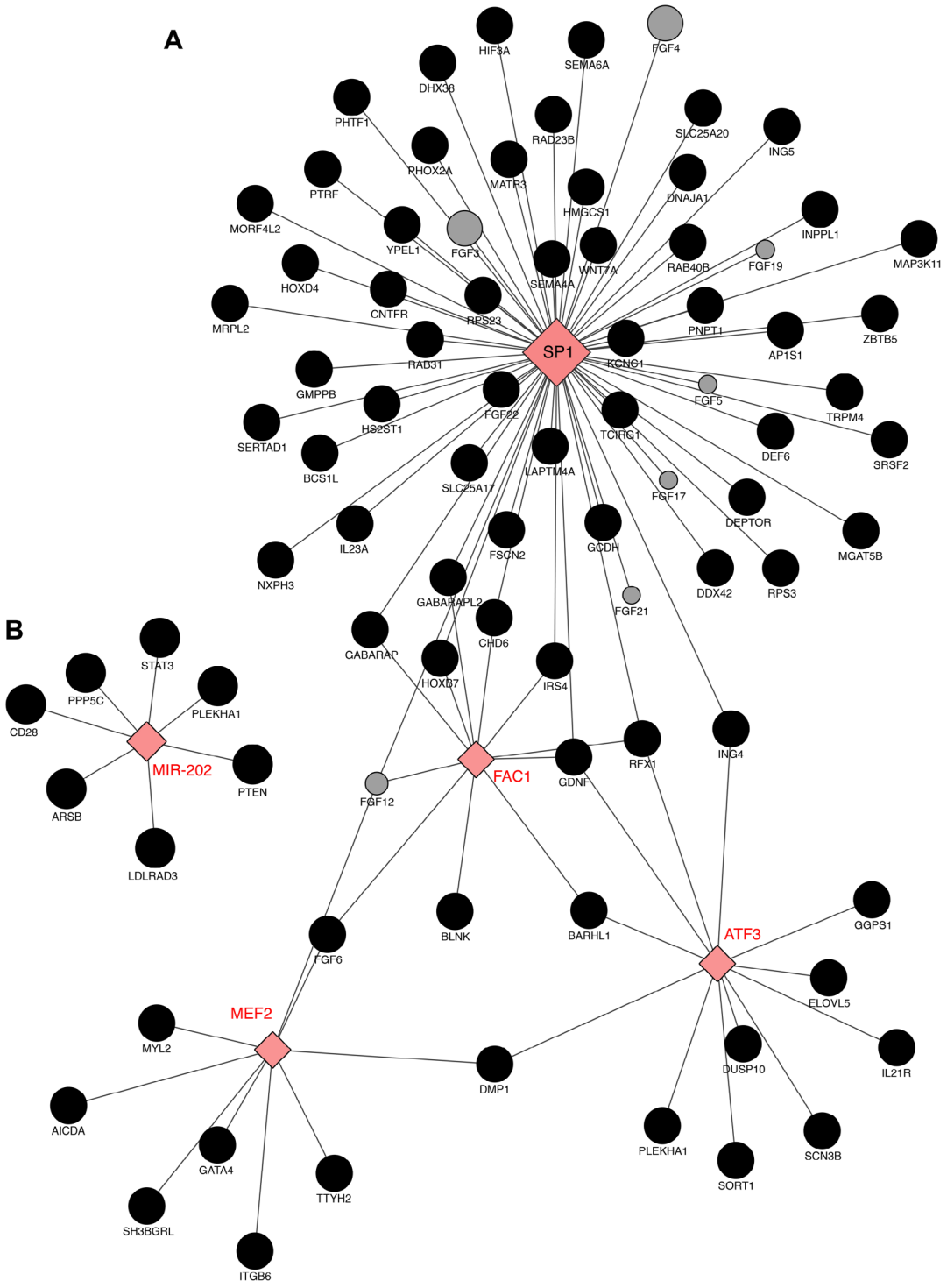

Figure S3. Transcription factor and microRNA binding sites enriched in axonal regeneration gene set (Related to Figure 3).

Analysis of the genomic sequences for the gene list in Figure 1 relative to Transcription Factor and microRNA binding sites from GeneMania (Montojo et al., 2010).

(A) Genes with genome-wide statistically significant (P<0.05) enrichment of binding sites for the transcription factors SP1, MEF2C, ATF3, and FAC1 within 2 kb of the ATG.

(B) Genes with genome-wide statistically significant (P<0.05) enrichment of binding sites for microRNAs in the 3'UTR, miR-202.

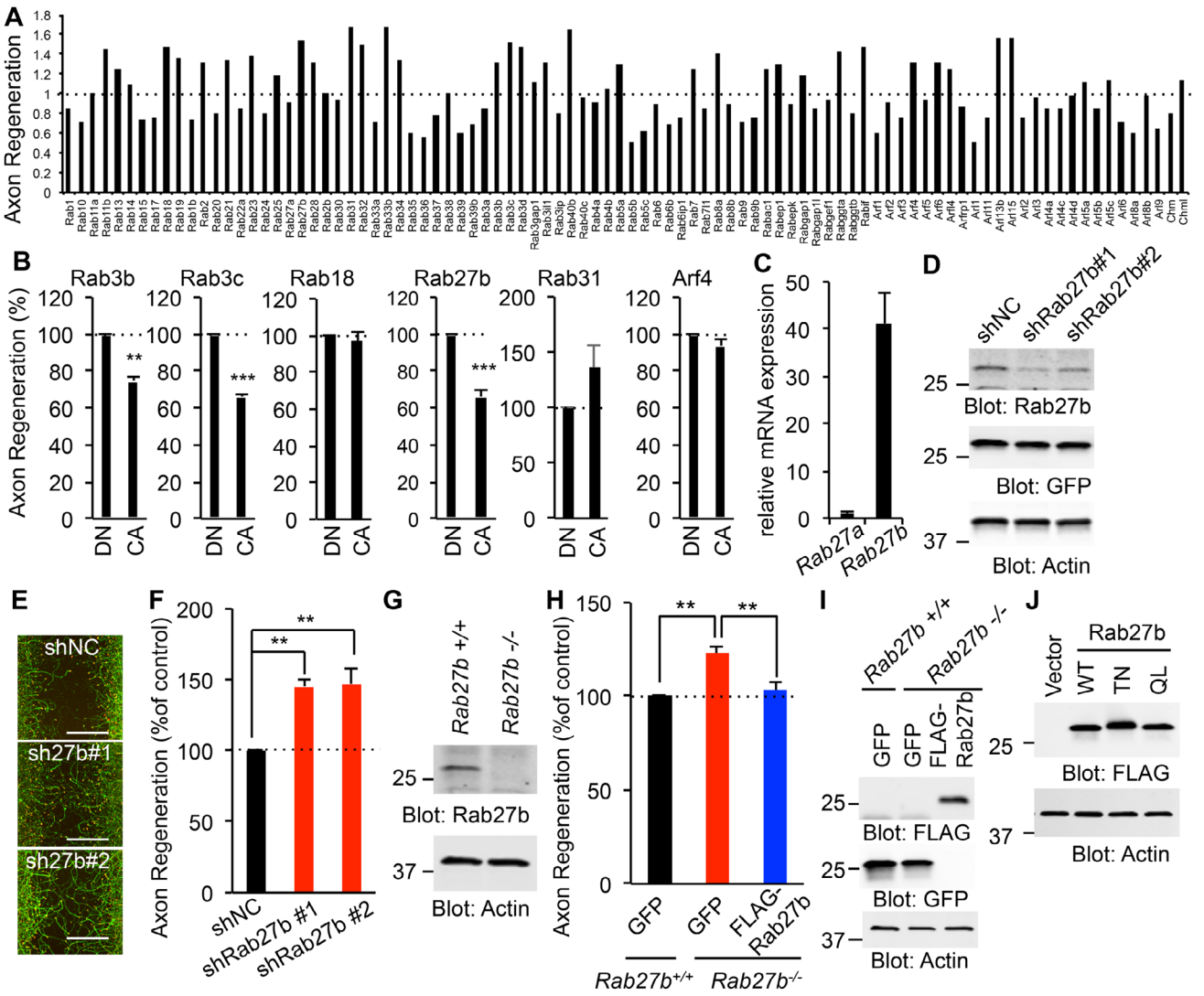

Figure S4. Rab related genes affecting axonal regeneration (Related to Figure 5).

(A) The summary of axonal regeneration of Rab and Rab related genes relative to control from full screen results. We put threshold at 1.3 for further retest study.

(B) Axonal regeneration assay was performed in dominant negative or constitutively active form of Rab3b, Rab3c, Rab18, Rab27b,Rab31 and Arf4 transfected neuron. Data are expressed as % of DN or Vector with SEM for n=3-4 biological replicates. **p<0.01, ***p<0.005, Student's t test.

(C) The comparison of *Rab27a* and *Rab27b* gene expression in DIV 10 cortical neuron. Data is *Rab27a* and *Rab27b* mRNA level normalized to those of a *beta-actin* internal control.

(D) The lysate from indicated shRNA construct nucleofected neurons was immunoblotted with indicated antibodies.

(E) Representative pictures of regenerated axons 3 days after axotomy stained with βIII tubulin (green) and phalloidin of F-actin (red). Cortical neurons were nucleofected with shNC, shRab27b#1 or #2. Scale bars represent 200 μm.

(F) The graph shows quantification of axonal regeneration % of shNC. Error bars represent SEM, n=4 biological replicates. **p<0.01, one-way ANOVA followed by Tukey's test.

(G) The lysate from *Rab27b*$^{+/+}$ or *Rab27b*$^{-/-}$ cortical neuron was immunoblotted with anti-Rab27b and Actin antibodies.

(H) Rescue experiment was performed in Rab27b-/- neuron transfected with GFP or FLAG-Rab27b. The graph shows quantification of axonal regeneration. Error bars represent SEM, n=4 biological replicates. **p<0.005, one-way ANOVA followed by Tukey's test.
(I) The lysate from *Rab27b*$^{+/+}$ cortical neuron nucleofected with GFP, *Rab27b*$^{-/-}$ cortical neuron nucleofected with GFP or FLAG-Rab27b WT was immunoblotted with anti-FLAG, GFP and Actin antibodies.
(J) The lysate from Vector, Rab27b WT, TN or QL nucleofected neurons was immunoblotted with anti-FLAG and Actin antibodies.

Figure S5. Rab27b expression in retina (Related to Figure 6).
(A) The lysate from *Rab27b*$^{+/+}$ or *Rab27b*$^{-/-}$ retina was immunoblotted with anti-Rab27b and Actin antibodies.
(B) The lysate from retina 3 days after optic nerve crush in WT mice (n=3) was immunoblotted with anti-Rab27b and Actin antibodies.
(C) Quantification of Rab27b protein levels in the lysates normalized to Actin. Mean±SE (n=3). No significant difference, Student's two-tailed *t* test.

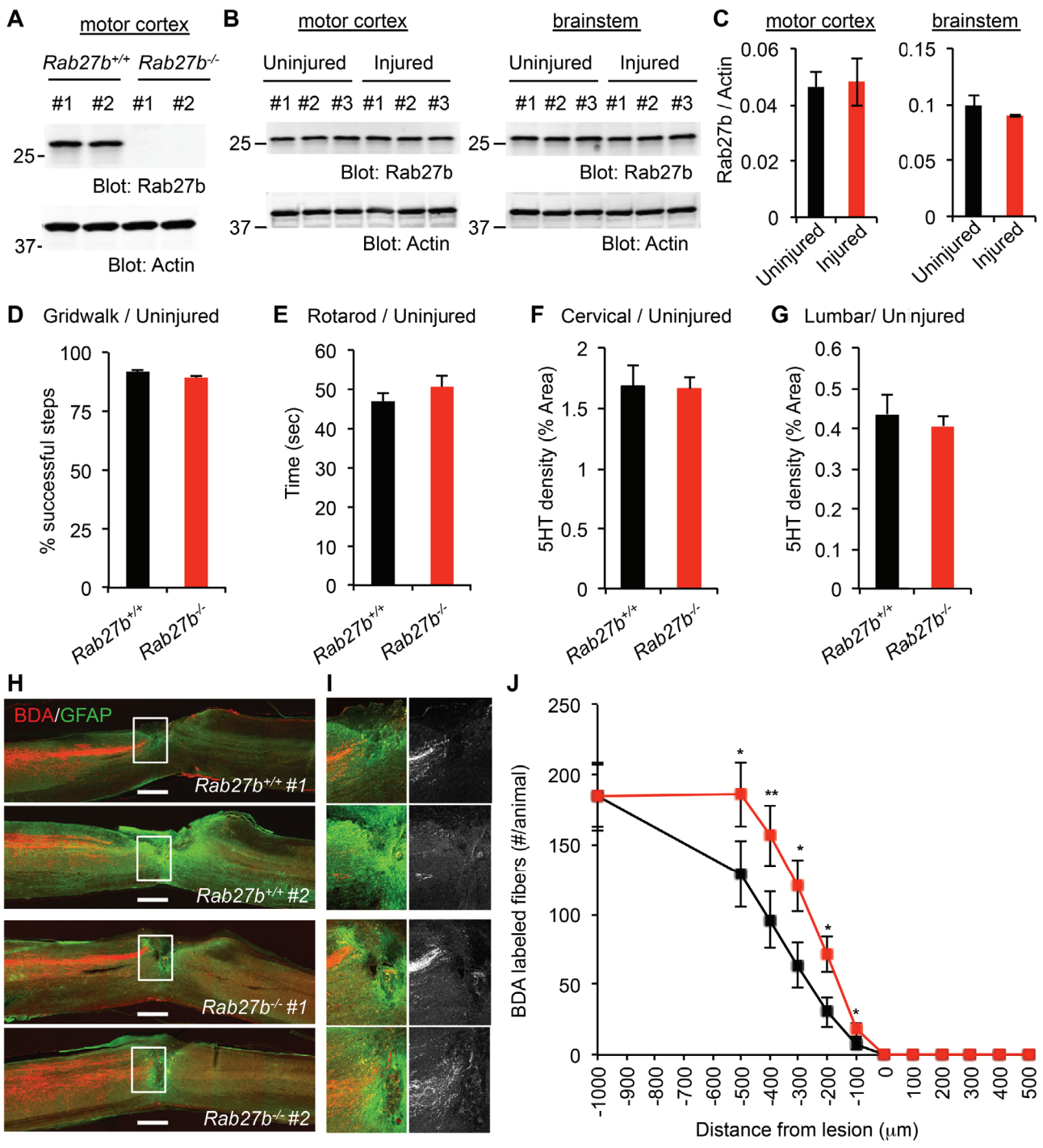

Figure S6. Characterization of Rab27b-/- mice without CNS trauma (Related to Figure 7).
(A) The lysate from *Rab27b*$^{+/+}$ or *Rab27b*$^{-/-}$ motor cortex was immunoblotted with anti-Rab27b and Actin antibodies.
(B) The lysates from motor cortex and brainstem 7 days after dorsal hemisection in WT mice (n=3) were immunoblotted with anti-Rab27b and Actin antibodies.
(C) Quantification of Rab27b protein levels in the lysates normalized to Actin. Mean±SE(n=3). No significant differences between groups with Student's two-tailed *t* test.

(D) Gridwalk test of *Rab27b*$^{+/+}$ and *Rab27b*$^{-/-}$ mice without spinal cord injury were assessed. Data are mean with SEM for n=4 *Rab27b*$^{+/+}$ and n=4 *Rab27b*$^{-/-}$. No significant differences between groups with Student's t test.
(E) RotaRod performance of *Rab27b*$^{+/+}$ and *Rab27b*$^{-/-}$ mice before spinal cord injury were assessed. Data are mean with SEM for n=19 *Rab27b*$^{+/+}$ and n=19 *Rab27b*$^{-/-}$. No significant differences between groups with Student's t test.
(F, G) Serotonergic (5HT+) fiber density at coronal sections of cervical and lumbar cord from uninjured *Rab27b*$^{+/+}$ and *Rab27b*$^{-/-}$ mice. Data are presented as mean with SEM for n=5 to 11 *Rab27b*$^{+/+}$ and *Rab27b*$^{-/-}$ animals. No significant differences between groups with Student's t test.
(H) Representative sagittal section from Rab27b+/+ and Rab27b-/- mouse. BDA was injected into the sensorimotor cortex at 8 weeks post injury and mice were killed 2 weeks later. Sections were visualized for BDA in red and GFAP in green; dorsal is up and rostral is left. Scale bar 500mm.
(I) The area in the white boxes from (F) is magnified.
(J) Quantification of BDA-labeled CST fibers rostral and caudal to the lesion site. BDA-labeled fibers are counted in every other section from each animal. Data are mean with SEM for n=19 *Rab27b*$^{+/+}$ and n=17 *Rab27b*$^{-/-}$. *p<0.05, **p<0.01, Student's t test.

REFERENCES

Basso, D.M., Fisher, L.C., Anderson, A.J., Jakeman, L.B., McTigue, D.M., and Popovich, P.G. (2006). Basso Mouse Scale for locomotion detects differences in recovery after spinal cord injury in five common mouse strains. Journal of neurotrauma *23*, 635-659.
Byrne, A.B., Edwards, T.J., and Hammarlund, M. (2011). In vivo laser axotomy in C. elegans. Journal of visualized experiments : JoVE.
Erturk, A., Mauch, C.P., Hellal, F., Forstner, F., Keck, T., Becker, K., Jahrling, N., Steffens, H., Richter, M., Hubener, M.*, et al.* (2011). Three-dimensional imaging of the unsectioned adult spinal cord to assess axon regeneration and glial responses after injury. Nat Med *18*, 166-171.
Fink, K.L., Lopez-Giraldez, F., Kim, I.J., Strittmatter, S.M., and Cafferty, W.B.J. (2017). Identification of Intrinsic Axon Growth Modulators for Intact CNS Neurons after Injury. Cell Rep *18*, 2687-2701.
Huebner, E.A., Kim, B.G., Duffy, P.J., Brown, R.H., and Strittmatter, S.M. (2011). A multi-domain fragment of Nogo-A protein is a potent inhibitor of cortical axon regeneration via Nogo receptor 1. The Journal of biological chemistry *286*, 18026-18036.
Mello, C., and Fire, A. (1995). DNA transformation. Methods Cell Biol *48*, 451-482.
Mello, C.C., Kramer, J.M., Stinchcomb, D., and Ambros, V. (1991). Efficient gene transfer in C.elegans: extrachromosomal maintenance and integration of transforming sequences. The EMBO journal *10*, 3959-3970.
Montojo, J., Zuberi, K., Rodriguez, H., Kazi, F., Wright, G., Donaldson, S.L., Morris, Q., and Bader, G.D. (2010). GeneMANIA Cytoscape plugin: fast gene function predictions on the desktop. Bioinformatics *26*, 2927-2928.
Starkey, M.L., Barritt, A.W., Yip, P.K., Davies, M., Hamers, F.P., McMahon, S.B., and Bradbury, E.J. (2005). Assessing behavioural function following a pyramidotomy lesion of the corticospinal tract in adult mice. Experimental neurology *195*, 524-539.
Tanabe, K., Bonilla, I., Winkles, J.A., and Strittmatter, S.M. (2003). Fibroblast growth factor-inducible-14 is induced in axotomized neurons and promotes neurite outgrowth. Journal of Neuroscience *23*, 9675-9686.
Tolmachova, T., Abrink, M., Futter, C.E., Authi, K.S., and Seabra, M.C. (2007). Rab27b regulates number and secretion of platelet dense granules. Proc Natl Acad Sci U S A *104*, 5872-5877.
Wang, X., Yigitkanli, K., Kim, C.Y., Sekine-Komo, T., Wirak, D., Frieden, E., Bhargava, A., Maynard, G., Cafferty, W.B., and Strittmatter, S.M. (2014). Human NgR-Fc decoy protein via lumbar intrathecal

bolus administration enhances recovery from rat spinal cord contusion. Journal of neurotrauma *31*, 1955-1966.
Zou, Y., Stagi, M., Wang, X., Yigitkanli, K., Siegel, C.S., Nakatsu, F., Cafferty, W.B., and Strittmatter, S.M. (2015). Gene-Silencing Screen for Mammalian Axon Regeneration Identifies Inpp5f (Sac2) as an Endogenous Suppressor of Repair after Spinal Cord Injury. J Neurosci *35*, 10429-10439.